International Journal of Electronics Communication and Computer Engineering
Volume 10, Issue 6, ISSN (Online): 2249–071X

An Enhanced Carrier Acquisition Algorithm for Low SNR and High Dynamic Signal

Almas Kaveh [1*], Liu Rongke [2] and Vahid Alipour Maralani [3]
[1] School of Electronic Information Engineering, Beihang University, Beijing 100191, China.
[2] School of Electronic Information Engineering, Beihang University, Beijing 100191, China.
[3] School of Electronic Information Engineering, Beihang University, Beijing 100191, China.
*Corresponding author email id: lb1602210@buaa.edu.cn

Date of publication (dd/mm/yyyy): 14/11/2019

***Abstract* – In deep space communications, the received signals have low SNR and high dynamic. The high dynamic characters cause a large Doppler frequency shift and frequency change rate so it makes to create problem in signal reception and processing. The traditional algorithm based on the maximum likelihood method for the carrier frequency acquisition with high dynamic and low SNR signal is analyzed. To solve this problem, an enhanced carrier acquisition algorithm with FFT and cyclic shifting accumulation by calculating periodogram, is proposed. There for by using this algorithm the signal frequency acquisition performance is enhanced. Also by the enhanced algorithm cyclically shifts the signal spectrum, the influence of the Doppler frequency change rate is eliminated, and then the captured carrier frequency accuracy is higher.**

***Keywords* – Maximum Likelihood, Deep Space Communication, High Dynamic, Low SNR.**

I. INTRODUCTION

Compared with the near-earth space communication, deep space communication is very far away and has very low SNR and other characteristics. At the same time, because of the large radial velocity and acceleration of the deep space detector, the received signal has high dynamic characteristics. Therefore cause a large Doppler frequency shift and frequency change rate. To achieve communication between the ground station and the detector during deep space exploration, first, the high dynamic and weak signal frequency acquisition problem must be solved. At present, there are many frequency acquisition methods for high dynamic weak signals. A frequency estimation algorithm based on linear predictor is given in [1], but the simulation is not performed under very low SNR conditions. Therefore, its conclusion is not applicable to deep space communication. In [2], the high-dynamic weak signal of the three algorithms based on the maximum likelihood method (ML) frequency estimation algorithm, the extended Kalman filter (EKF) based frequency estimation algorithm and the crossover frequency automatic control loop algorithm, the frequency estimation performance is compared. The conclusion is that the frequency estimation algorithm based on the maximum likelihood method is more suitable for the frequency estimation of high dynamic and weak signals, but the computational complexity is not optimized because the maximum likelihood method is not used in this paper.

Literature [3] proposed a cross-fuzzy function method combined with $Zoom\ FFT$ estimation of Doppler dynamics, which achieves accurate estimation of signal Doppler dynamics with low complexity, but this method is only suitable for Doppler frequency offset. The situation, and the SNR should reach $-10dB$ or more. In some papers, a multi-branch time-domain change rate matching FFT modulus selection large frequency estimation algorithm is used, which can capture the Doppler frequency and its first-order rate of change under low SNR conditions, but the time domain required by the method the rate of change matching accuracy is high, so the matching branch data required under high dynamic conditions is huge, resulting in an extremely large amount of calculation, which limits the practical use of the method. In [4], a maximum likelihood algorithm based on periodic

map is proposed. Compared with other methods, the matching accuracy requirement of Doppler rate of change is reduced. Under the same dynamic conditions, the amounts of calculation are reduced.

In this paper, the algorithm principle of the literature [4] is studied. It is found that there is a Doppler frequency change rate difference between each sub-data segment when the average period spectrum is obtained, which leads to the non-coherent accumulation not achieving the best performance. Based on this, an enhanced algorithm for frequency domain cyclic shifting accumulation and periodogram calculation is proposed. This algorithm effectively enhances the frequency acquisition performance of the algorithm.

II. Frequency Estimation Based on Maximum Likelihood

In deep space communication, the received signal by the front-end receiver is down-converted. The frequency components include the intermediate frequency, the Doppler frequency, the Doppler frequency change rate, and the higher-order rate of change. In the capture phase, the rate of change of the second order and above of the Doppler frequency is not considered [4], so the received signal can be analyzed using the constant rate of change model. Without loss of generality, the intermediate frequency is zero, and the complex form of the received signal is:

$$r(t) = A \cdot \exp\left(j \cdot (2\pi f_d t + \pi a t^2)\right) + n(t) \quad (1)$$

In the formula, $A = \pm 1$ is the modulation information, f_d is the Doppler frequency, a is the Doppler frequency change rate, and $n(t)$ is the additive white Gaussian noise with a mean value of σ^2.

The method for estimating the carrier Doppler frequency f_d and the Doppler frequency change rate a in deep space communication is a frequency estimation method based on the maximum likelihood method [4]. The capture process of the signal frequency is essentially that the search process of the carrier frequency space and the carrier frequency change rate space, is multiplying the input signal by a different frequency change rate in the assumed N_r frequency change rate space,

$$x_l(t) = r(t) \cdot \exp(-j\pi \hat{a}_l t^2) \quad 0 \le t \le T, 1 \le l \le N_r \quad (2)$$

Where $\hat{a}$ represents the carrier frequency change rate in the frequency change rate space of the l hypothesis, and T is the duration of the input signal $r(t)$. The obtained $x_l(t)$ is divided into M consecutive sub-data segments, and each sub-data segment has a time length of $\Delta T = T/M$. Each sub-data segment is separately subjected to FFT transformation, and the sum of the squares of the amplitudes obtained by the FFT transformation is averaged to obtain an estimated amount $P_l(f_k), 1 \le l \le N_r, f_k = k/\Delta T, -N_{FFT}/2 + 1 \le k \le N_{FFT}/2$ of the periodic graph. Finally, based on the branch and frequency index of the maximum value of $P_l(f_k)$, the estimated values of Doppler frequency and Doppler frequency change rate $\hat{f}_d$ and $\hat{a}$ are obtained. The principle of the algorithm is shown in Figure1.

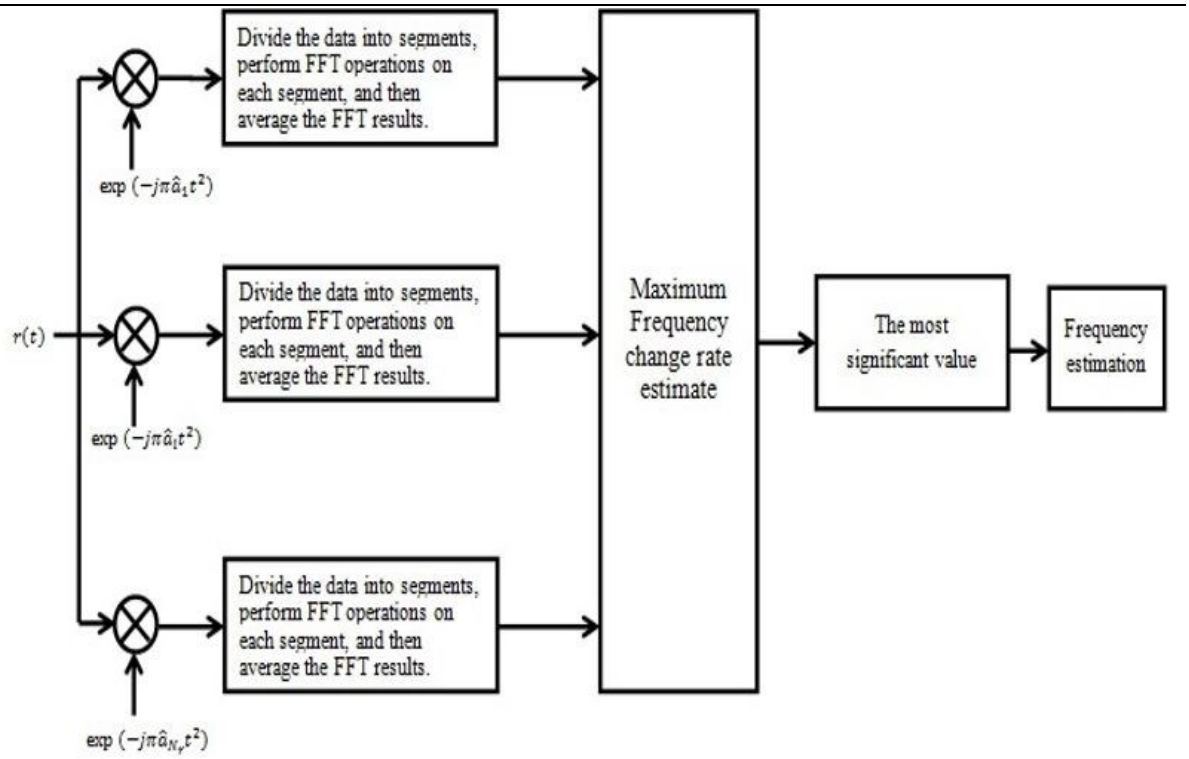

Fig1. Block diagram of carrier estimation based on maximum likelihood method

The input signal is multiplied by the preset Doppler frequency change rate of each branch. When the Doppler frequency change rate of a branch is closest to the actual Doppler frequency change rate, the average of the branch is obtained. The maximum peak value appears in the periodogram, and the position of the maximum value is the estimated frequency. The Doppler frequency change rate preset by the branch is the estimated Doppler frequency change rate. By Combining formula (1) and (2):

$$x_l(t) = r(t) \cdot \exp(-j\pi \hat{a}_l t^2) = A \cdot \exp\left(j(2\pi f_d t + \pi \Delta a_l t^2)\right) + n(t) \cdot \exp(-j\pi \hat{a}_l t^2) \quad (3)$$

Where Δa_l is the difference in frequency change rate of the branch, $\Delta a_l = a - \hat{a}_l$. The signal power spectrum with Doppler frequency change rate is close to the rectangle when the time bandwidth product B. $T_s \gg 1$ ($T_s$is the sampling time interval and B is the signal bandwidth) [5]. When FFT is obtained for the signal with the difference of the frequency change rate, T_s is shorter, and the bandwidth of the frequency change rate difference is less than the time window bandwidth $2/T_s$. The Fourier transform of the m ($m = 1,2,\dots,M$) sub-data segment of the l branch is

$$X_l(f, m) = \int_{-\infty}^{+\infty} x_l(\tau) h(\tau) e^{-j2\pi f \tau} d\tau = \int_0^{T_s} x_l(\tau) e^{-j2\pi f \tau} d\tau \quad (4)$$

$$X_l(f, m) = AT_s \cdot S_a\left(\left(f - (f_d + \Delta a_l m T_s)\right)T_s\right) \cdot e^{-j\left(f - (f_d + \Delta a_l m T_s)\right)T_s} + N \quad (5)$$

Where $h(\tau)$, is a rectangular window of width T_s and N represents the noise term. It can be seen from equation (5) that due to the frequency change rate difference Δa_l, the peak value of the FFT transform results of different sub-data segments of each branch is not necessarily at the same frequency point, the larger Δa_l is, the larger the deviation of each peak is, which leads to the non-coherent accumulation of the M-segment signal spectrum and the optimal effect cannot be achieved.

III. ENHANCE ACQUISITION ALGORITHM

The aim of analysis of the algorithmic disadvantages in Section 2 of this paper, propose an enhanced algorithm for frequency domain cyclic shifting accumulation and calculating periodogram. In the virtual frame of Figure 1, the average periodogram is obtained. The spectrum of the first sub-data segment remains unchanged, and the remaining segments are cyclically shifted according to the values of Δa_l and m ($m = 2, \dots, M$), and then cyclically shifted. The square of the absolute value of the spectrum of each sub-data segment is non-coherently accumulated. Next, the number of points S_m in which the spectrum of each sub-data segment is cyclically shifted is derived. The sampling frequency used by the algorithm is f_s, the number of points for each sub-data segment to be FFT transformed is N_{FFT}, and the resolution of the FFT transform is f_s/N_{FFT}. The DFT absolute value of the m ($m = 1, 2, \dots, M$) sub-data segment of the branch l is obtained by equation (5). In the equation:

$$|DFT_l(K, m)| = |AN_s \cdot S_m(K - (k_d + \Delta a_l m N_s)N_s)| \tag{6}$$

In the formula, N_s is the number of points in timeT_s , and k_d is the Doppler frequency offset. After doing $S_m$point cyclic shift, equation (7) becomes

$$|\mathrm{DFT_l(K, m)}| = |\mathrm{AN_s \cdot S_a(K - (k_d + \Delta a_l m N_s + S_m \cdot f_s/N_{FFT})N_s)}| \tag{7}$$

To eliminate the offset of the spectrum of each sub-data segment caused by Δa_l, the $\Delta a_l m N_s + S_m . f_s/N_{FFT}$ term in equation (7) needs to be zero. The enhanced algorithm aims to shift the spectral peak of each sub-data segment to the peak of the first segment of the spectrum, and the number of points moved is an integer, so:

$$\mathrm{S_m = round\left(\Delta a_l \times (m - 1) \times \frac{N_s \times N_{FFT}}{f_s}\right)} \tag{8}$$

Where Round (·) represents the rounding operation, $m = 2, \dots, M$. The direction of the cyclic shift is related to the symbol of Δa_l when the actual frequency change rate is less than the preset frequency change rate, it is shifted to the left; otherwise, and it is shifted to the right.

It can be seen from equation (8) that the number of points of the cyclic shifting and the frequency change rate difference Δa_l, the sub-data segment is proportional to the position of the first sub-data segment $(m - 1)$, the number of points taken in the time T_S, and the frequency resolution f_s/N_{FFT} in inverse proportion. The larger the difference between the actual Doppler frequency change rate and the preset frequency change rate (less than the resolution of the frequency change rate), the peak value of each sub-data segment before the cyclic shifting is smaller than the peak value of the first sub-data segment. The larger the shift, is the larger the number of points to be cyclically shifted in the enhanced algorithm. Compared with the original algorithm, the spectral peak after cyclic shifting non-coherent accumulation is greatly enhanced.

When using the enhanced algorithm to find the periodogram, on the basis of the original algorithm, the calculation of the shift point number and the corresponding shift operation are added. It can be known from equation (8) that four multiplication operations and one shift operation are added when each sub-data segment is obtained, so the enhanced algorithm performs $4(M - 1)$ multiplication operations each time the periodic graph is obtained, with $(M - 1)$ shift operations. Since the M value in the algorithm is not large, the enhanced algorithm only slightly increases the complexity of the algorithm.

IV. SIMULATION

Parameter Settings

In the simulation, the simulation parameters of the system, including the sampling frequency f_s, FFT points N_{FFT}, Non-coherent accumulation times M, etc., need to be properly set according to signal characteristics and system performance requirements. Let the Doppler frequency range be $[f_{dmin}, f_{dmax}]$, the Doppler frequency change rate range be $[a_{min}, a_{max}]$, the Doppler frequency resolution be f_{dres}, the Doppler frequency change rate resolution be a_{res}, and the capture probability should be above 90%. Under the same system parameters, the simulation compares the performance of the original algorithm and the enhanced algorithm. The following is a selection of the selection principles for several major simulation parameters.

Sampling frequency f_s: Under the premise that the intermediate frequency is zero, the sampling frequency should ensure that the signals in the Doppler frequency range can be sampled, that is, satisfy the Nyquist sampling theorem $f_s \geq 2(f_{dmax} - f_{dmin})$. This paper takes the minimum value that satisfies the Nyquist sampling theorem, that is, twice the Doppler frequency range.

FFT points N_{FFT}: The frequency accuracy of the signal frequency capture stage should be able to meet the signal accuracy requirements of the latter stage tracking stage, and the tracking stage's requirement for Doppler frequency accuracy is the accuracy to be achieved by the FFT resolution, i.e. $f_{dres} = f_s/N_{FFT}$, hence $N_{FFT} = f_s/f_{dres}$.

Signal duration T: In the carrier frequency acquisition phase, the parameters of the second order and above of the Doppler frequency change rate are ignored, and the processing is based on the second order of the Doppler frequency change rate and the order above it in time T. The parameter value is so small that the Doppler frequency change rate can be regarded as a constant in time T.

Non-coherent accumulation times$M$: In order to increase the probability of acquisition, in addition to increasing the power spectrum peak as much as possible, the noise power spectrum variance should be minimized. Because the power spectrum variance is proportional to $1/M$, multiple accumulations can effectively reduce the noise power spectrum. However, the actual M cannot be infinitely large, and under the condition that the sampling ratef_s, the time T, and the FFT point number N_{FFT} are all determined, $M = f_s \cdot T/N_{FFT}$.

Simulation Results

Taking the entry phase of the Mars rover of the US Challenger as an example [4], the carrier-to-noise ratio varies within the range of $17dB - Hz \sim 20dB - Hz$, the Doppler frequency $f_d$varies by $-50kHz \sim 50kHz$, and the Doppler frequency change rate a is$0 \sim 800\,Hz/s$. The tracking phase requires carrier Doppler frequency acquisition accuracy to reach $f_{dres} \leq 20Hz$, and the accuracy requirement for Doppler frequency change rate is $a \leq 80\,Hz/s$. According to the analysis of the parameter setting in Section 4.1, set the sampling frequency $f_s = 200kHz$, FFTpoint $N_{FFT} = 10000$,the signal duration $T = 1s$, and the non-coherent accumulation number $M = 20$. Figure 2 shows the carrier acquisition probability P_a simulated by the original algorithm and the enhanced algorithm under different carrier-to-noise ratio conditions. 1000 simulations are performed under each carrier-to-noise ratio condition, and the results are statistically analyzed. It can be seen from Fig. 2 that under the same capture probability conditions, the carrier noise required by the enhanced algorithm is lower than the original

algorithm by $1dB - Hz \sim 2dB - Hz$. The enhanced algorithm improves the capture performance of the signal carrier frequency.

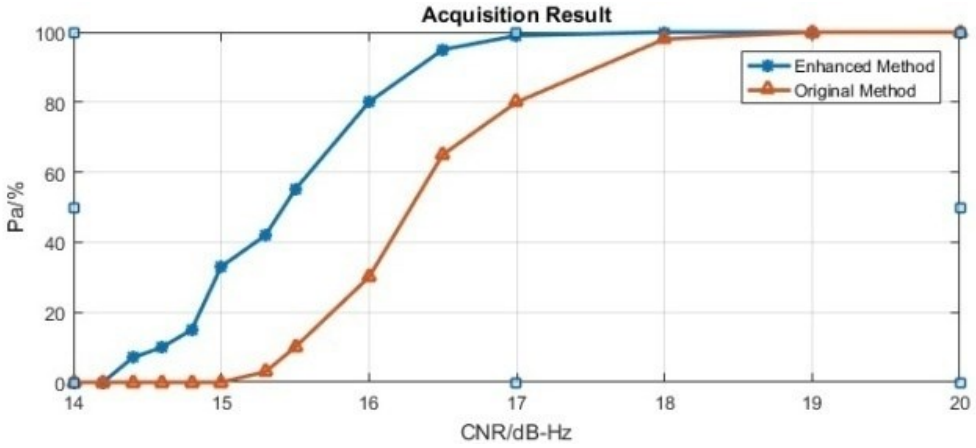

Fig. 2. Acquisition probabilities of original method in compare with the enhanced method with different CNR.

There is noise in the input signal. When the noise is relatively large, the capture result may be false alarm. Figure 3 shows the false alarm probability of the original algorithm and the enhanced algorithm under different carrier-to-noise ratio conditions. It can be seen from Fig. 3 that under the same carrier-to-noise ratio condition, the false alarm probability of the enhanced algorithm is reduced. Because the enhanced algorithm cyclically shifts the signal spectrum, the influence of the Doppler frequency change rate difference is eliminated, so the captured carrier frequency accuracy is higher.

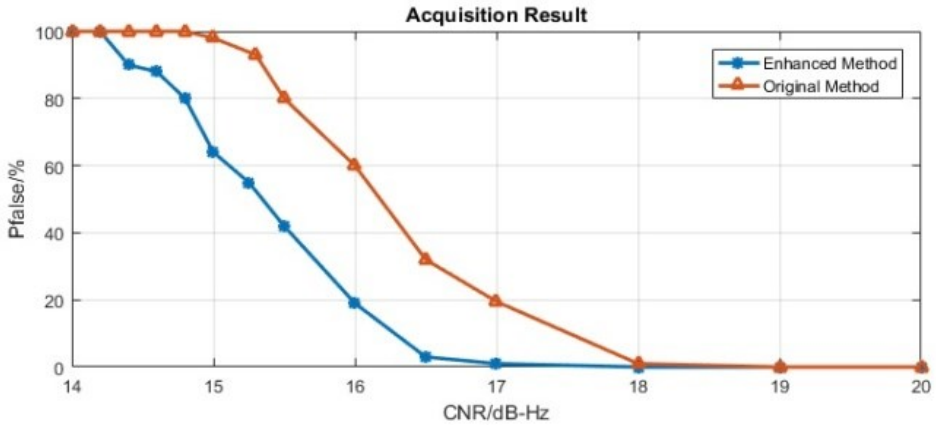

Fig. 3. False alarm probabilities of original method and enhanced method with different CNR

Table 1. Acquisition and False alarm probabilities of original method in comparison with the enhanced method with different CNR.

CNR (dB-Hz)	Original Method (Pa %)	Enhanced Method (Pa %)	Original Method (P False %)	Enhanced Method (P False %)
14	0	0	100	100
15	0	33	97	64
16	32	80	60	20
17	80	99	20	1
18	98	100	1	0
19	100	100	0	0

Figure 4 shows the standard deviation of the Doppler frequency and the actual Doppler frequency captured under different carrier-to-noise ratio conditions. It can be seen from the figure that the simulation results are consistent with the theoretical analysis.

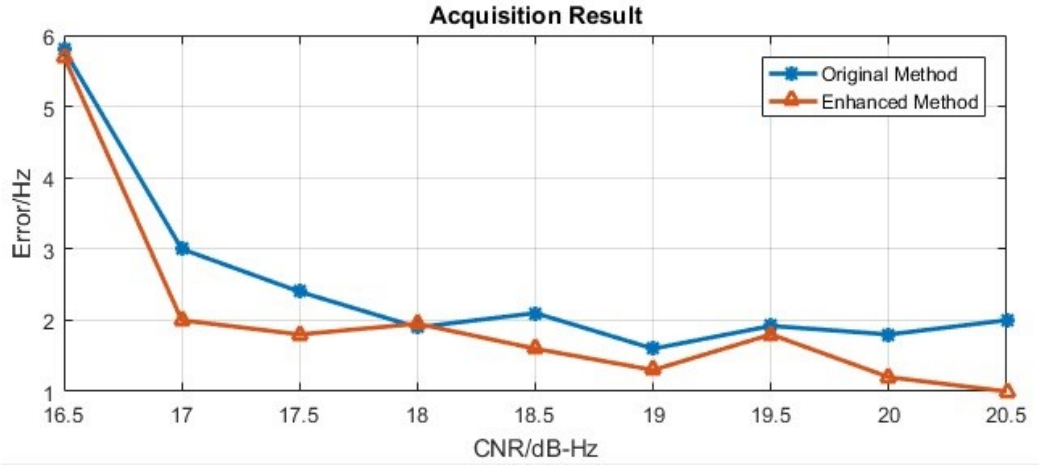

Fig. 4. Estimation error of Doppler frequency with different CNR.

Table 2 shows the comparison of estimation error of Doppler frequency from 17dB-Hz to 20.5dB-Hz with two methods as original and enhanced methods. According to table2, the error of enhanced method is better than the original one about 0.1 to 1 Hz.

Table 2. Estimation error of Doppler frequency in different CNR by Original method and Enhanced method.

CNR (dB-Hz)	Original Method (Error/Hz)	Enhanced Method (Error/Hz)
17	3	2
17.5	2.5	1.9
18	2	2
18.5	2.1	1.6
19	1.6	1.3
19.5	1.9	1.8
20	1.8	1.2
20.5	2	1

V. CONCLUSION

In this paper, we study the deep-space high dynamic weak signal frequency acquisition algorithm based on the maximum likelihood method, and find that there is a frequency difference between each sub-data segment when averaging the periodogram. Aiming at this problem, this paper proposes a frequency domain cyclic shift accumulating periodic graph algorithm, and deduces the relationship between the number of cyclic shift points and frequency resolution. Finally, the correctness and effectiveness of the enhanced algorithm are verified by simulation.

REFERENCES

[1] Jackson L.B., Tufts D.W., Soong F.K., and Rao R.M. Frequency Estimation by Linear Prediction [C] IEEE International Conference on ICASSP, 1978: 352～356.

[2] Vilnrotter V.A., Hinedi S, Kumar R. Frequency Estimation Techniques for High Dynamic Trajectories [J]. IEEE Transactions on Aerospace and Electronic Systems, 1989.
[3] Ma S.X., Jiang J.N., Meng Q. A Fast, Accurate and Robust Method for Joint Estimation of Frequency and Frequency Rate [C] IEEE International Symposium on Intelligent Signal Processing and Communication Systems (ISPACS 2011), 2011.
[4] Satorius E, Estabrook P, Wilson J and Fort D. Direct to Each Communication and Signal Processing for Mars Exploration Rover Entry, Descentand Landing [R]. IPN Progress Report, 2003, 42~153.
[5] Cowell D.M.J. Freear S. Separation of Overlapping Linear Frequency Modulated (LFM) Signals using the Fractional Fourier Transform [J]. IEEE Transactions on Ultrasonic, Ferroelectrics and Frequency Control, 2010, 2324~2333.

AUTHOR'S PROFILE

Almas Kaveh, Electronic Engineer BS graduated from Khaje Nasir Aldin Toosi University-Tehran Iran and received Master Degree of Global Navigation Satellite System from Beihang University-Beijing China. He is doctoral student of satellite communication in Beihang University. email id:lb1602210@buaa.edu.cn.

Rongke Liu, received the B.S. and Ph.D. degrees from Beihang University, Beijing, China, in 1996 and 2002, respectively. He was a Visiting Professor with the Florida Institution of Technology, USA, in 2005; The University of Tokyo, Japan, in 2015; and the University of Edinburgh, U.K., in 2018, respectively. He is currently a Full Professor with the School of Electronics and Information Engineering, Beihang University. He received the support of the New Century Excellent Talents Program from the Minister of Education, China. He has attended many special programs, such as China Terrestrial Digital Broadcast Standard. He has authored/coauthored more than 100 papers in international conferences and journals. email id: rongke_liu@buaa.edu.cn.

Vahid Alipour Maralani, finished his bachelor degree in electrical engineering (2010), then pursue MSc and Received master degree from Beihang University in the field of Global Navigation Satellite System (2014). Now he is researcher in field of GNSS. email id: vahidalipour@buaa.edu.cn.